Magnetic Properties of Ferromagnetic Quasi-1D Copper-Peptide Compounds: Exchange Interactions and Very Low Temperature Phase Transitions

Edson F. Chagas,[†] Raul E. Rapp,*[,†] Daniel E. Rodrigues,[‡] Nieves M. C. Casado,[‡] and Rafael Calvo*[,‡]

Instituto de Física, Universidade Federal do Rio de Janeiro, CP 68528, Rio de Janeiro 21941-972, RJ, Brazil, and Departamento de Física, Facultad de Bioquímica y Ciencias Biológicas, Universidad Nacional del Litoral, and INTEC (CONICET−UNL), Güemes 3450, 3000 Santa Fe, Argentina

Received: November 24, 2005; In Final Form: February 22, 2006

The magnetic properties of the Cu(II)−peptide compounds (L-tyrosyl-L-leucinato)Cu(II) and (L-tryptophyl-glycinato)Cu(II), to be identified as Cu(II)Tyr-Leu and Cu(II)Trp-Gly, respectively, have been investigated by specific heat ($0.08 < T < 28$ K), dc magnetization ($2 < T < 80$ K, with $B_0 = \mu_o H \leq 9$ T), and ac magnetic susceptibility (with $B_0 = 0$ for $0.03 < T < 3$ K and B_0 up to 9 T for $2 < T < 80$ K) measurements. Above ~1 K, the specific heat and magnetization of both compounds display a ferromagnetic (FM) spin chain behavior sustained by syn-anti carboxylate bridges connecting equatorially Cu(II) ions at about 5 Å. To model this behavior, we calculated the eigenvalues of Heisenberg chains with up to 20 spins $^1/_2$ and used the method of Bonner and Fisher. A global fit of the model to the specific heat and magnetization data gives $2J_0/k_B = 3.60(5)$ K and 2.59(5) K for the intrachain exchange interactions in Cu(II)Tyr-Leu and Cu(II)Trp-Gly, respectively ($\mathcal{H}_{ex}(i,j) = -2J_0\ \mathbf{S}_i \cdot \mathbf{S}_j$). These values of $2J_0$ are discussed in terms of structural properties of the carboxylate bridges in the two compounds. Using the parameters obtained from the global fit, we calculated isothermal susceptibilities in agreement with the ac susceptibilities measured with small applied dc magnetic fields. However, the ac susceptibility measured with applied dc fields larger than 1 T lie between the values calculated for the isothermal and adiabatic susceptibilities. At 0.16 K for Cu(II)Tyr-Leu and 0.53 K for Cu(II)Trp-Gly, the observed specific heat and magnetic susceptibility display peaks associated to three-dimensional magnetic phase transitions. The interchain exchange couplings $2J_1$ producing the 3D magnetic order are ferromagnetic and have magnitudes $2J_1/k_B \sim 0.015$ and 0.073 K for Cu(II)Tyr-Leu and Cu(II)Trp-Gly, respectively.

Introduction

Low dimensional magnetic behavior of real compounds is usually a consequence of large differences between the magnitudes of the exchange couplings between neighboring magnetic ions located in different directions.[1] Because of the greater simplicity, experimental and theoretical studies of chain systems have been important to test many-body theories on magnetism,[2] to observe quantum effects and short-range magnetic order, and to evaluate the exchange couplings between neighbor spins in the chain from experimental results.[3,4] Since the pioneering works of Bonner and Fisher[3] and Griffiths[5] on the thermodynamic properties of Heisenberg spin chains, many real quasi-1D compounds have been discovered and investigated.[1]

Superexchange interactions[6] are transmitted through chemical bridges containing one or more diamagnetic atoms connecting the unpaired electrons. Important advances were done in the past decades in correlating the magnitudes of these interactions to the structure of the bridges.[1] Carboxylate bonds, one of the best-studied superexchange bridges, have a highly versatile behavior. A strong antiferromagnet (AFM) exchange coupling ($2J_0/k_B = -480$ K) was observed in copper acetate,[7] a binuclear complex where four symmetry-related syn-syn acetate groups bridge two copper ions at 2.616 Å. Ferromagnetic (FM) and AFM interactions transmitted through the less symmetric and weaker syn-anti carboxylate bridges have been reported in clustered and in polymeric copper compounds.[8−19] Colacio et al.[10,15] and other authors[17,19] showed that the magnitude and even the sign of the exchange interaction strongly depend on the molecular and electronic structure of the bridge. Structural and magnetic studies of FM helix−like Cu(II) spin chains provided by syn-anti carboxylate bridges have been reported.[11,15] The common structural features of these compounds, acting as tridentate toward a copper ion and as monodentate toward the next copper in the chain, were described by Freeman et al.[20] The Cambridge Crystallographic Database[21,22] contains more than twenty copper(II)−peptide compounds having these syn-anti carboxylate bridges. Several of them, e.g., those studied in this work, show in addition good magnetic isolation between copper chains. The characterization of some of these chain systems has been made by susceptibility measurements at relatively high temperatures.[11,13−15,17,19] Thus, the accuracy of the calculated exchange interactions is low, being difficult to compare results for compounds with similar structures. In addition, the dependence of the values of the susceptibility and magnetization with the magnitudes of small exchange interactions is weak and has an additional cross-correlated dependence with the *g*-factor of the magnetic ion. This fact indicates the

* Corresponding authors: calvo@fbcb.unl.edu.ar, Phone/FAX +54 342 460-8200. rapp@if.ufrj.br, Phone +55 21 2562 7666, FAX +55 21 2562 7368.

[†] Universidade Federal do Rio de Janeiro.

[‡] Universidad Nacional del Litoral.

10.1021/jp056838w CCC: $30.25
Published on Web 03/31/2006

convenience of having other sources of magnetic information in order to study magnetostructural correlations of spin chains.

Bonner and Fisher[3] evaluated the thermodynamic properties of finite Heisenberg chains using the eigenvalues of chains with N_S spins and extrapolating the results to the thermodynamic limit, $N_S \rightarrow \infty$. The lowest temperatures where these predictions are valid depend on the value of N_S,[3,23] and the quality of the calculated thermodynamic properties improves using eigenvalues for chains with increasing length. Bonner and Fisher[3] used $N_S \leq 11$ spins and studied AFM and FM spins. Fabricius et al.[24] extended N_S to 16 and studied AFM chains; Costa-Filho et al.[17] used their eigenvalues to calculate the magnetization and susceptibility of FM chains.

The Hamiltonian $\mathscr{H}$ for a uniform Heisenberg chain with N_S isotropic spins and nearest neighbor exchange interactions under a magnetic field B applied along $\boldsymbol{z}$ is

$$\mathscr{H} = |J_0|\tilde{\mathrm{H}} \tag{1}$$

with

$$\tilde{\mathrm{H}} = \tilde{\mathrm{H}}_{ex} + \tilde{\mathrm{H}}_z = -2\frac{J_0}{|J_0|}\sum_{i=1}^{N_S}\mathbf{S}_i\cdot\mathbf{S}_{i+1} + \sum_{i=1}^{N_S} y\mathrm{S}_{i,z} \tag{2}$$

where in eqs 1 and 2, $J_0 > 0$ for FM interactions, $\tilde{\mathrm{H}}$ and $\tilde{\mathrm{H}}_z$ are scaled isotropic exchange and Zeeman interactions, respectively, and $y = g\mu_B B/|J_0|$. Most experimental and theoretical efforts have been done with AFM chains.[1,5,25−27] Those for FM chains have been lagging because of the fewer realizations and because they have higher difficulties (see later).

Recently we reported measurements of magnetization and ac magnetic susceptibility in the presence of applied dc magnetic fields for the compound Cu(II)Trp-Gly.[17] Our results allowed progress in the understanding of the problem but showed a failure to fully explain the observed ac susceptibility in the presence of large dc magnetic fields. The absence of other type of data (e.g., specific heat measurements) restricted the possibility of a full characterization of the syn-anti carboxylate bridges as superexchange paths. Here we report a complete set of specific heat, magnetization, and susceptibility measurements for the copper complexes of the dipeptides L-tyrosyl-L-leucine and L-tryptophyl-glycine, where syn-anti carboxylate bridges connect copper ions along chains. Our experimental results cover a wide range of temperature above and below the region in which short range order takes place, allowing full identification of the one-dimensional magnetic behavior and also observing at very low temperatures transitions to phases with three-dimensional (3D) long-range magnetic order.

We found useful for this work and for future calculations to obtain the eigenvalues of chains with 17−20 spins with periodic boundary conditions and use them to calculate the thermodynamic properties of FM chains in a wide temperature range. We also discuss the ac susceptibility observed in the presence of an external dc field. The observed phase transitions, consequence of weak exchange interactions transmitted through long biological relevant chemical bridges containing H-bonds[28,29] or cation-π interactions,[30,31] are discussed within the spin-wave approximation.[32,33] The transition temperatures and the behavior of the specific heat below the transition allow to estimate interchain exchange interactions in agreement with values recently obtained from single-crystal electron paramagnetic resonance (EPR) measurements of Cu(II)Tyr-Leu[34,35] and of Cu(II)Trp-Gly.[17]

Experimental Section

Materials Preparation. The preparation and crystal structures of the copper−dipeptide complexes (L-tyrosyl-L-leucinato)-copper(II),[34,36] $C_{15}H_{19}CuN_2O_4$, and (L-tryptophyl-glycinato)-copper(II),[17,37] $C_{13}H_{13}CuN_3O_3$, identified as Cu(II)Tyr-Leu and Cu(II)Trp-Gly, respectively, have been reported before.

Specific Heat Measurements. Specific heat measurements were made using two calorimeters. One, mounted in a dilution refrigerator cryostat (model DRI-420, SHE Corporation) covers the temperature range 0.08−2 K.[38] The other, mounted in a ^{3}He cryostat (Janis Research Co.), covers the range 0.5−28 K.[39] Both calorimeters use a semi adiabatic pulse method with essentially the same acquisition system. The temperature resolution is between 0.01 and 0.05% and the specific heat uncertainty is ∼2%.

The samples were prepared as to improve the low thermal conductivity of the material.[38,40] Powdered samples, with particle size of ∼100 μm, were mixed with powdered copper, with particle size of ∼5 μm. The sample−copper mixtures were wrapped with 0.04 mm thick copper foil, forming a chip, which was compressed with 37 MPa for ∼10 min. The chips were glued with Apiezon N grease to the copper plate of the calorimeter base, where the thermometer and heater are attached. The mass of the samples, copper, and grease addenda were about 0.1, 0.2, and 0.002 g, respectively. These samples have good thermal conducting copper paths around particles and a thermal equilibration time constant shorter than 60 s in the full measuring range, maintaining small the specific heat background due to the added material. This procedure facilitates fast replacements and allows using the same sample in both calorimeters. When taking data, heat was applied to the sample during intervals of about 100 seconds to produce temperature changes between 0.5 and 5% of the sample temperature. The evolution to equilibrium of the temperature of the sample was monitored during more than 500 s. The specific heat background of the calorimeter was determined in a separate measurement. The total heat capacity of the sample, C_{exp}, was obtained subtracting from the measured value the heat capacity of the calorimeter and the contributions of the copper powder and foil,[41] and the Apiezon N grease.[42]

Magnetic Measurements. Magnetization and ac susceptibility measurements of powder samples of about 0.04 g were made in the temperature range $2 < T < 80$ K in a PPMS with the ACMS option (Quantum Design, Inc.), and applied magnetic fields up to $B_0 = \mu_o H = 9$ T (μ_o is the vacuum permeability). The sample holder was made of Rexolite (C-Lec Plastics, Inc.) whose magnetic moment at the magnetic fields used for the samples is small and negative, with strong magnetic field dependence and was subtracted from the data. This sample holder displays a magnetization peak at about 55 K which becomes important for large applied magnetic fields. It is in a temperature region outside of the range of interest of our measurements and was subtracted from the data by measuring a similar empty holder.

The ac susceptibility at temperatures $0.03 < T < 4$ K was measured with a homemade susceptometer mounted in the mixing chamber of the dilution refrigerator. A cylinder made of Stycast 1266 (Emerson and Cuming, Inc.) supports the primary and two secondary coils wound in opposition, all made of copper wire. Thermalization is obtained by grounding to the mixing chamber one extreme of copper "coil foil" (a sheet of parallel thin copper wires glued with General Electric 7031 varnish) embedded in the Stycast. Powder samples of ∼0.015 g were packed inside small cylinders made of Rexolite (3 mm

TABLE 1: Values of the Intrachain and Interchain Exchange Parameters, $2J_0$ and $2J_1$, and the *g* Factor Calculated with a Global Fitting of the Model to the Magnetization and Thermal Data[a]

	Cu(II)(Tyr-Leu)	Cu(II)(Trp-Gly)
$2J_0/k_B$ (K)	3.60(5)	2.59(5)
$2J_1/k_B$ (K)	0.015(2)	0.073(5)
g	2.112(2)	2.090(1)
$\|2J_1\|/k_B$ (K) (EPR)	0.016(1)[b]	0.061(2)[c]
g_{AV} (EPR)	2.108	2.094
bridge	Cu O4 C11 O3 Cu	Cu O1 C2 O2 Cu
d (Cu−Cu)	4.980 Å	5.147 Å
d′ (along the bond	6.390 Å	6.422 Å
O−C−O angle	123.16	124.55
torsion angles	−0.41°, 175.95°	16.54°, 176.08°

[a] The value of $|2J_1|$ obtained from EPR experiments is included for comparison. The last two rows contain structural results. [b] References 34, 35. [c] Reference 17.

diameter, 0.2 mm wall, and 5 mm height), which were placed into an independent sample holder made of Stycast and "coil foil" grounded to the mixing chamber for thermalization and positioned in the center of one of the secondary coils. Measurements of the ac susceptibility at very low *T* were performed at $\nu = 250$ and 500 Hz with an ac magnetic field $B_{ac} \sim 0.01$ mT. The output $\kappa(T)$ of the susceptometer is related to the susceptibility of the sample, $\chi(T)$, by

$$\kappa(T) = \alpha + \beta\,\chi(T) \tag{3}$$

We evaluated α and β of eq 3 by comparing $\kappa(T)$ measured with the very low *T* susceptometer with $\chi(T)$ measured with the PPMS (used as a patron) between 2 and 4 K. The values of β obtained for different samples are very similar; α varies about 15%. Thus, the calibration using eq 3 was repeated for each sample. Unfortunately, below 0.5 K the temperature equilibrium time between sample and mixing chamber becomes important because the sample, a poor thermal conductor, is in vacuum and inside of a plastic cylinder. As a result, the temperature difference between sample and thermometer could be significant and we do not obtain good temperature accuracy. Thus, we will not make precise comparisons of the temperature for the specific heat and susceptibility measurements in the very low *T* region.

Diamagnetic contributions[1,25] $\chi_d = -1.67 \times 10^{-4}$cm^3/mol and -1.55×10^{-4} cm^3/mol for Cu(II)Tyr-Leu and Cu(II)Trp-Gly are already subtracted from the magnetization and susceptibility data presented below.

Crystal Structure and Exchange Pathways

Cu(II)Tyr-Leu[36] and Cu(II)Trp-Gly[37] crystallize in the orthorhombic space group $P2_12_12_1$ with four rotated molecules (labeled as A, B, C, and D)[43] per unit cell. The Cu(II) ions are in helical chains, along the *a*-axis in Cu(II)Tyr-Leu, and along the *b*-axis in Cu(II)Trp-Gly (Figures 1a and 2a). Neighbor copper ions in a chain, at 4.98 Å in Cu(II)Tyr-Leu and at 5.14 Å in Cu(II)Trp-Gly, are connected by similar syn-anti carboxylate bridges between equatorial oxygen ligands. These bridges (total bond lengths 6.39 Å and 6.42 Å) support the exchange interactions between neighbor coppers in a chain. The structural parameters of the carboxylate bridges are given in Table 1. The main difference between these bridges for Cu(II)Tyr-Leu and Cu(II)Trp-Gly is in one of the torsion angles (angle between the plane defined by the carboxylate O−C−O bond and the direction of the Cu−O bond), which varies from −0.4° for Cu(II)Tyr-Leu to 16.6° for Cu(II)Trp-Gly, indicating a nearly planar bridge for Cu(II)Tyr-Leu and a large deviation from the plane for Cu(II)Trp-Gly.

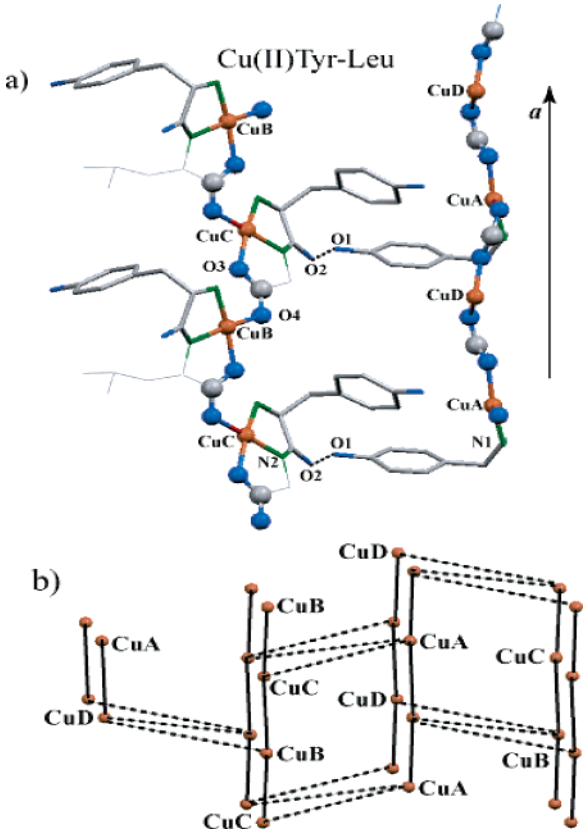

Figure 1. Molecular structure of Cu(II)Tyr-Leu (from ref 36). A, B, C, and D indicate rotated molecules in the unit cell. (a) The left side shows a Cu chain made of atoms CuB and CuC (distance d(CuB − CuC) = d(CuA − CuD) = 4.98 Å), coupled by equatorial−equatorial syn-anti carboxylate bridges CuC−O3−C−O4−CuB (total bond length 6.39 Å). On the right side there is a neighbor chain made of copper atoms CuA and CuD. An interchain chemical path connecting CuA and CuC atoms in neighbor chains is displayed. (b) Network of chemical paths connecting coppers ions. Thick solid lines represent carboxylate bridges connecting coppers along the chains. Dashed lines represent interchain paths connecting copper ions with two coppers in neighbor chains.

Figures 1a and 2a include a symmetry related copper chain and describe the relevant interchain connections between neighbor copper ions. In the case of Cu(II)Tyr-Leu (see Figure 1a), copper atoms at $d = 9.73$ Å in neighbor chains are connected equatorially by long chemical bridges containing 12 diamagnetic atoms, including a strong hydrogen bond (total bond length $d' = 19.12$ Å).[36] The bridge providing the strongest exchange interaction path interconnecting spin chains in Cu(II)Tyr-Leu is shown in Figure 3a. In the case of Cu(II)Trp-Gly (see Figure 2a and ref 37) there are two different bridging systems connecting copper ions at 10.53 Å (path I) and at 7.53 Å (path II) in neighbor spin chains (shown in Figures 3b and 3c), both containing a cation-π contact[30,31] between a copper ion and the indole ring of a tryptophan residue at its apical positions.[17,37] Path I contains one bridge of seven atoms; path II is a bridging system containing two bridges, one with six atoms and the cation-π contact and other with five diamagnetic atoms, including one hydrogen bond. The distances between the copper ions and the closest carbon atom of the indole rings producing the cation-π contact are d(C8−Cu)= 3.234 Å and d(C11−Cu)= 3.548 Å for paths I and II, respectively. Thus, the shorter cation-π contact in path I is expected to be stronger than that in path II.

The intra- and interchain superexchange interaction networks connecting neighbor copper chains in Cu(II)Tyr-Leu and in

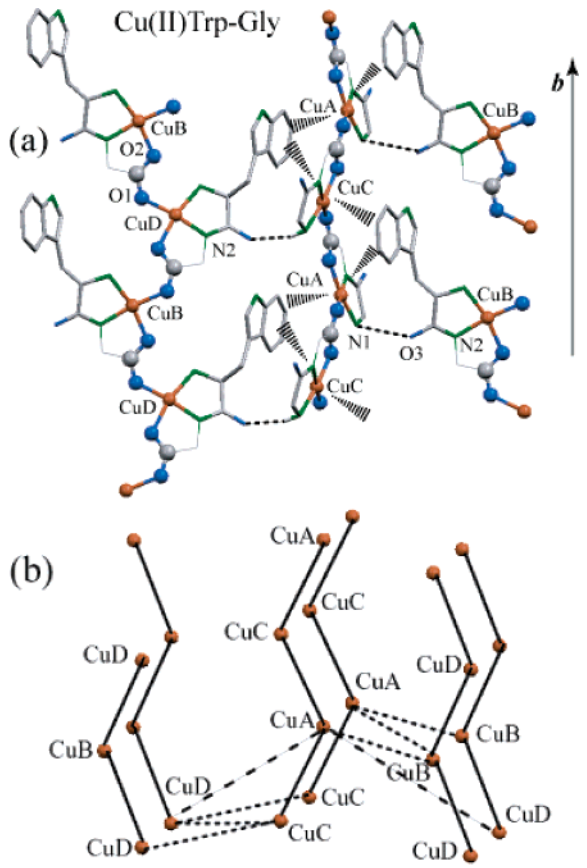

Figure 2. Molecular structure of Cu(II)Trp−Gly (from ref 37). A, B, C, and D indicate rotated molecules in the unit cell. (a) The left side shows a Cu chain made of atoms CuB and CuD (distance d(CuB − CuD) = d(CuA − CuC) = 5.15 Å), connected by equatorial−equatorial carboxylate bridges CuB−O2−C−O1−CuD (total bond length 6.422 Å). On the right side there is a neighbor chain made of copper atoms CuA and CuC. There are interchain chemical paths of two types, both including cation−π contacts. (b) Network of chemical paths connecting copper ions. Thick solid lines represent carboxylate bridges connecting coppers along the chains. Long-dashed lines represent paths type I connecting neighbor chains. Short-dashed lines represent paths type II. Each copper is connected to two coppers in neighbor chains by paths type I, and to other two by paths type II.

Cu(II)Trp-Gly are described in Figures 1b and 2b. In both cases a copper ion is connected to two copper neighbors in the chain by the syn-anti carboxylate bridges. In Cu(II)Tyr-Leu, each copper is also connected to two coppers in different neighbor chains by symmetry related paths shown in Figure 3a. The next copper ion in the chain is connected to two coppers in other chains in the other side. In Cu(II)Trp-Gly each copper is connected to two coppers in neighbor chains through paths I, and to other two coppers in other neighbor chains through the supposedly weaker paths type II. The final result for Cu(II)-Trp-Gly is similar to that for Cu(II)Tyr-Leu, and the exchange network produces a weak interconnection in the plane perpendicular to the chains that is responsible for 3-D order. We call $2J_0$ the intrachain exchange interactions (see eqs 1 and 2) sustained by the carboxylate bridges and $2J_1$ the interchain interactions supported by the long chemical paths containing H-bonds [Cu(II)Tyr-Leu] or cation-π contacts [Cu(II)Trp-Gly].

Experimental Results

Specific Heat Data. The values of the molar specific heat, $C_{exp}(T)$, measured for Cu(II)Tyr-Leu and Cu(II)Trp-Gly in the two different cryostats are displayed in Figures 4a,b, respectively, in units of $R = N_{Av}k_B = 8.3145$ J/(mol K). A good agreement between the values obtained in the two calorimeters in the overlapping range $0.5 < T < 2$ K reflects the quality of the measurements.

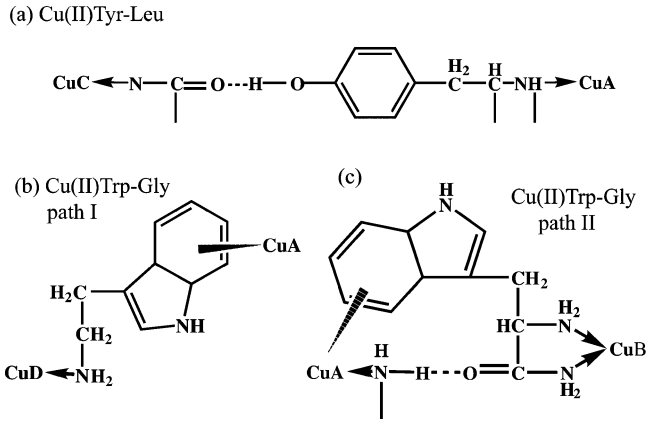

Figure 3. Exchange chemical bridges connecting coppers in neighbor chains. (a) Bridge made of 12 atoms, including one hydrogen bond, connecting CuA and CuC and CuB to CuD copper ions at $d = 9.73$ Å in Cu(II)Tyr-Leu (total bond length $d' = 19.09$ Å). (b) Path I connecting CuA to CuD atoms at $d = 10.53$ Å in Cu(II)Trp-Gly. It contains seven atoms and a cation−π contact (contact length $d(C_{11}-Cu) = 3.234$ Å; total bond length $d' = 14.01$ Å). (c) Path II, connecting CuA to CuB coppers at $d = 7.53$ Å in Cu(II)Trp-Gly, is a bridging system with two bridges. One contains six atoms and a cation−π contact (contact length $d(C_8-Cu) = 3.548$ Å; total bond length $d' = 9.442$Å). The other contains five atoms, including an H-bond.

The temperature dependence of C_{exp} of both compounds display three main qualitative facts. At high temperatures the magnitude is dominated by the vibrational contribution which will be subtracted (see below). At intermediate temperatures there is a broad peak with a maximum value $(C_{mag}/R)_{max} \sim 0.14$. Considering the chain structure of the copper ions, this peak indicates the approach of the spin chains to short-range magnetic order; the observed maximum value of C_{mag}/R proves[3] that this order is FM. For Cu(II)Trp-Gly, this result agrees with that reached from magnetic measurements.[17] The third qualitative fact are the narrow peaks of C_{mag}/R observed in Figures 4a,b at $T = 0.16$ K and at 0.53 K for Cu(II)Tyr-Leu and Cu(II)-Trp-Gly, respectively, indicating transitions to phases with 3D magnetic order. For Cu(II)Tyr-Leu wide and narrow peaks are well separated; for Cu(II)Trp-Gly they partially overlap. Figure 5a displays in logarithmic scale the specific heat peaks observed in the low T range.

$C_{exp}(T)$ is the sum of a magnetic contribution, $C_{mag}(T)$, and a vibrational (phonon) contribution, $C_{vib}(T)$. To obtain $C_{mag}(T)$, we approximated $C_{vib}(T)$ by a function containing odd powers of T:[44]

$$C_{vib}(T) = \sum_{k=1}^{m} a_k T^{2k+1} \qquad (4)$$

To evaluate the parameters a_k for each compound we fitted the equation

$$C_{exp}(T) = C_{vib}(T) + C_{mag}^{1D}(T) \qquad (5)$$

to the experimental values of C_{exp} considering terms up to $m = 4$. These expressions were fitted to the data in Figures 4a,b at temperatures above T_{1D} ($T_{1D} = 1.66$ and 1.68 K for Cu(II)Tyr-Leu and Cu(II)Trp-Gly, respectively), where the magnetic contribution to the specific heat can be described by a 1D model.

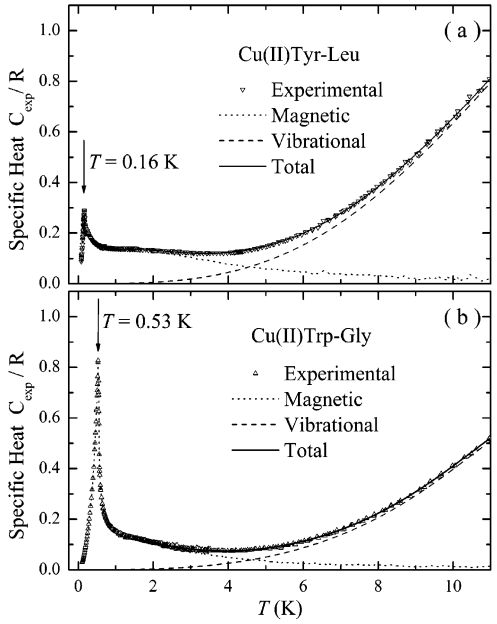

Figure 4. Heat capacity of (a) Cu(II)Tyr-Leu, (b) Cu(II)Trp-Gly, measured with the two calorimeters in the low- and very-low-temperature range. In addition to the experimental points (triangles), also displayed are the magnetic and lattice contributions calculated using eqs 5 and A1, as explained in the text.

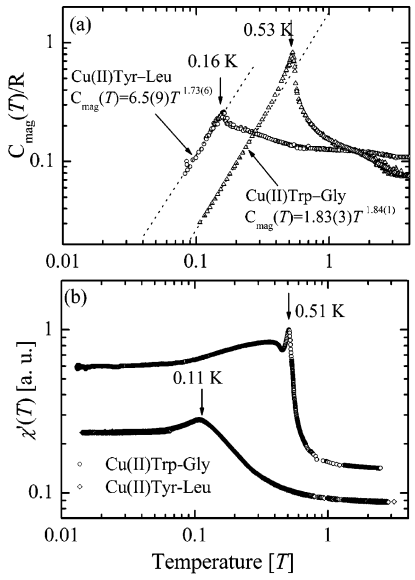

Figure 5. (a) log−log plot of the molar specific heat of Cu(II)Tyr-Leu and Cu(II)Trp-Gly as a function of temperature emphasizing the peaks at 0.16 K for Cu(II)Tyr-Leu and at 0.53 K for Cu(II)Trp-Gly) associated with 3D magnetic phase transitions. (b) log−log plot of the molar ac susceptibility of Cu(II)Tyr-Leu and Cu(II)Trp-Gly as a function of temperature.

Using smaller values of T_{1D} the standard deviations of the fittings become larger. The magnetic contribution to the specific heat is described by a 1D model in a later section. Appendix 1 provides an accurate functional expression of $C_{mag}^{1D}(T)$ for an FM chain with nearest neighbor interactions, valid in a wide range of temperatures. Equations 4 and 5 are more accurate than proposing T dependences of C_{mag}^{1D}(T) and $C_{vib}(T)$ at high temperatures proportional to $T^{-\gamma}$ and T^3, respectively.[25,44] The values obtained for the coefficients of eq 4 are $a_1 = (5.6\pm0.2) \times 10^{-3}$ J/(K^{4}mol), $a_2 = (1.9\pm0.5) \times 10^{-5}$ J/(K^{6}mol), $a_3 = (-3.1\pm0.5) \times 10^{-7}$ J/(K^{8}mol), and $a_4 = (10\pm2) \times 10^{-10}$ J/(K^{10}mol) for Cu(II)Tyr-Leu, and $a_1 = (3.41\pm0.08) \times 10^{-3}$ J/(K^{4}mol), $a_2 = (-5\pm4) \times 10^{-6}$ J/(K^{6}mol), $a_3 = (1.1\pm0.6) \times 10^{-7}$ J/(K^{8}mol), and $a_4 = (-7\pm2) \times 10^{-10}$ J/(K^{10}mol) for Cu(II)-Trp-Gly. They indicate Debye temperatures[33] $\theta_D = (70.4\pm0.7)$ K and (82.9 ± 0.7) K for Cu(II)Tyr-Leu and Cu(II)Trp-Gly, respectively. These fittings of eq 5 to the specific heat data give also values $2J_0/k_B = (3.7\pm0.1)$ K and (2.6 ± 0.1) K for the intrachain exchange parameters of Cu(II)Tyr-Leu and Cu(II)-Trp-Gly, respectively. The magnetic contribution C_{mag} to the specific heat of Cu(II)Tyr-Leu and of Cu(II)Trp-Gly in the whole range of T was obtained subtracting C_{vib} from C_{exp}. The values of $C_{vib}(T)$ and $C_{mag}(T)$ obtained by this procedure are plotted in Figs. 4a,b. These values of $C_{mag}(T)$ are used later for a global fit of a 1D magnetic model to the thermal and magnetization data. The procedure used above reduces the uncertainty of $C_{mag}(T)$ introduced by the vibrational contribution to the specific heat.

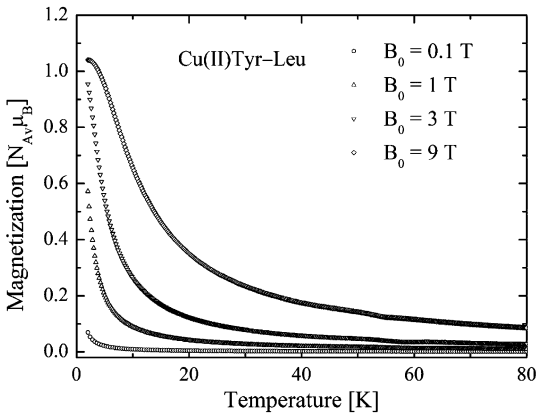

Figure 6. Magnetization measurements as a function of temperature for Cu(II)Tyr-Leu (see ref 45). Similar data for Cu(II)Trp-Gly were published in ref 17.

Magnetization and Susceptibility Data. The magnetization of Cu(II)Tyr-Leu is shown in Figure 6.[45] That for Cu(II)Trp-Gly was reported previously.[17] Figures 7a,b display the static magnetic susceptibility χ_o obtained for Cu(II)Tyr-Leu and Cu(II)Trp-Gly from the magnetization data at $B_0 = 0.3$ T. The values of $\chi'(T)$ obtained with a dc magnetic field of 0.3 T, also included in Figure 7a,b, are equal within the experimental uncertainties to $\chi_o(T)$. The ac susceptibility measured for Cu(II)-Tyr-Leu as a function of temperature in the range 2−80 K with applied dc magnetic fields $B_0 = 0.1$, 0.3, 1, 3, and 9 T, and ac excitation field $B_{ac} = 1$ mT are essentially frequency independent at $\nu = 100$, 1000, and 10000 Hz. These measurements were performed with the dc magnetic field applied after cooling the sample to the lowest temperature in zero field (ZFC). Similar susceptibility measurements were reported before for Cu(II)-Trp-Gly.[17] Both sets of results for the real contribution χ' at 1000 Hz are shown in Figures 8a,b. The observed imaginary part of the susceptibility χ'' is 2 orders of magnitude smaller than χ' and close to the uncertainty of the measurements. The ac susceptibilities of Cu(II)Tyr-Leu and Cu(II)Trp-Gly measured in the temperature range $0.03 < T < 3$ K, at 250 and 500 Hz with $B_{ac} = 0.01$ mT and $B_0 = 0$ using the low T susceptometer are also nearly frequency independent, and $\chi'' \ll \chi'$. Figure 5b displays the values of χ' obtained at 250 Hz for both samples. At low T they show the 3D magnetic phase transitions as wide peaks at temperatures shifted to lower temperatures from those observed in the specific heat data. These shifts may not reflect a temperature shift of the peaks, but rather a temperature difference between sample and thermometer. The best values for the transition temperatures are those given by the specific heat data.

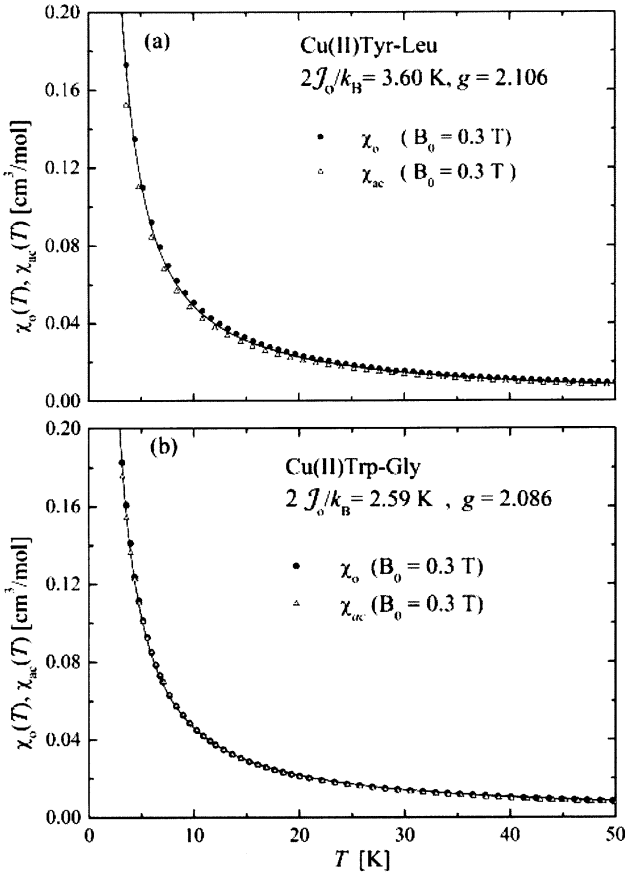

Figure 7. Experimental values of the static magnetic susceptibility χ_o and the ac magnetic susceptibility χ' measured for $B_0 = 0.3$ T compared with the predictions (solid lines) obtained with eq 11 for (a) Cu(II)-Tyr-Leu and (b) Cu(II)Trp-Gly. To avoid cluttering, only one-fifth of the experimental points are displayed.

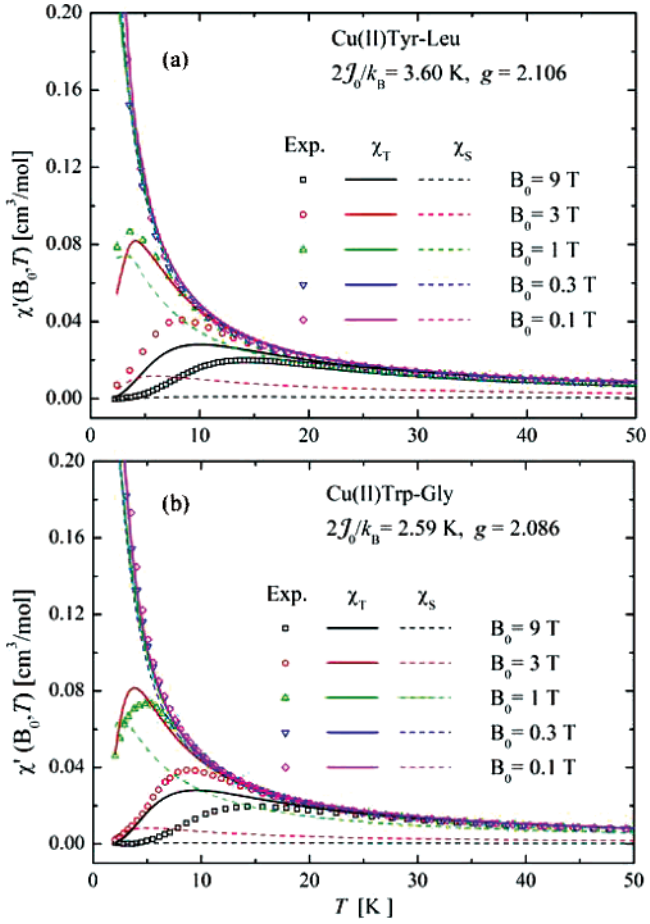

Figure 8. ac magnetic susceptibility $\chi'(T)$ measured (circles) as a function of temperature in the presence of a dc magnetic field for (a) Cu(II)Tyr-Leu and (b) Cu(II)Trp-Gly. They are compared with isothermal (solid lines) and adiabatic (dashed lines) susceptibilities calculated using eqs 11, A4, and A5. To avoid cluttering, only one-sixth of the experimental points are displayed. Symbols and lines with the same color are used for each value of the applied magnetic field.

Analysis of the Results

Global Fitting of the Specific Heat and Magnetization Data. The molar magnetic contribution to the specific heat C_{mag} of a chain at temperature T and magnetic field B_0 ($B_0 = 0$ for our specific heat data) is given by

$$\frac{C_{mag}(B_0,T)}{R} = \frac{1}{N_S(k_BT)^2}[\langle \mathscr{H}^2\rangle - \langle \mathscr{H}\rangle^2] \qquad (6)$$

The molar magnetization operator $\mathscr{M}_z$ and its statistical value $M_z(B_0,T)$ along the direction of the applied field B_0 for chains of N_S isotropic spins in units of μ_B are given by

$$\frac{\mathscr{M}_z}{N_{Av}\mu_B} = -\frac{g}{N_S}\sum_{i=1}^{n} S_{i,z} \qquad (7)$$

$$M_z(B_0,T) = \langle \mathscr{M}_z\rangle \qquad (8)$$

$\langle \mathscr{H}\rangle$ and $\langle \mathscr{H}^2\rangle$ in eq 6 and $\langle \mathscr{M}_z\rangle$ in eq 8 are mean values of the Hamiltonian of eqs 1 and 2 and the magnetization of eq 7, calculated over the $n = 2^{N_S}$ eigenstates of an N_S spins chain. The specific heat and magnetization in the T range with predominant 1D behavior will be calculated as a function of $2J_0$ and g, using the method of Bonner and Fisher[3] and eqs 1, 2, 6, 7, and 8.

The specific heat and magnetization for finite AFM chains with odd and even number of spins approach the limit for $N_S = \infty$ from both sides, allowing high accuracy in the extrapolation. FM chains approach these limiting values from one side,[3] and longer chains are required to obtain equal accuracy in the extrapolation. We calculated in this work the eigenvalues E_i of chains with up to 20 spins $^1/_2$ using an improved algorithm and a binary algebra procedure to efficiently deal with the many zero matrix elements of the Hamiltonian. The dispersion of the eigenvalues corresponding to the degenerate S^2 multiplets for each q arising from numerical errors is $|\delta E_i/E_i| < 2 \times 10^{-5}$. To force expected degeneracies and reducing the numerical errors, degenerate eigenvalues were averaged. Using these results we calculated as a function of $x = k_BT/|J_0|$ and of $y = g\mu_BB/|J_0|$ (see eqs 1 and 2), and extrapolated to infinite chains[3,23,24] the molar specific heat (eq 6) and magnetization (eqs 7 and 8) needed to fit the experimental data. Figure 9 shows the results for the specific heat of FM chains with 20 spins. Our results for chains of up to 16 spins are equal to those previously reported.[3,17,26,24] Increasing the length of the chain beyond $N_S = 16$ clearly produces a better description of the specific heat at temperatures close and below that where the maximum value occurs (see inset of Figure 9).

Considering basic concepts in ferromagnetism,[32] Bonner and Fisher,[3] Blöte,[26] and de Neef et al.[23] proposed that $C_{mag}^{1D} \propto T^{1/2}$ in the very low temperature range, where calculations with finite chains are not valid. De Neef[23] also used a polynomial in x with three half integer terms ($x^{1/2}$, $x^{3/2}$, and $x^{5/2}$) to extrapolate intermediate temperature results to lower temperatures where

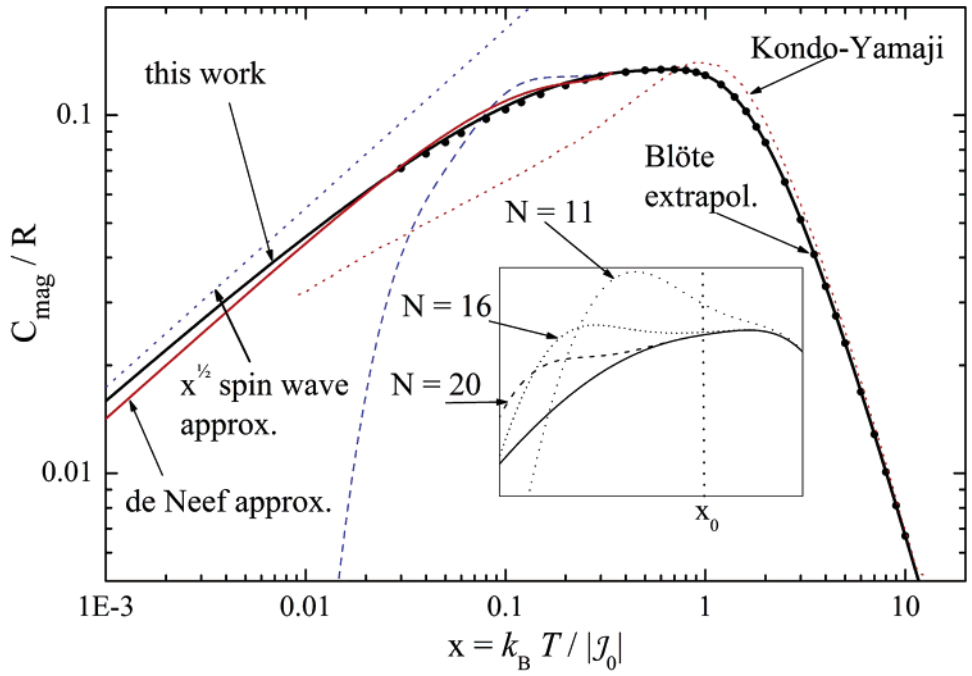

Figure 9. log−log plot of the values of the specific heat of FM spin chains in the range $0.001 < x = k_BT/|J_0| < 10$ (solid black line) calculated as explained in the text with finite chains of 20 spins for $x > x_o = 0.466$ and using eq 9 for $x < x_o$. These results are compared with those calculated by Blöte[26] (black dots), by Kondo and Yamaji[48] (dotted red line), and by de Neef[23] (solid red line). The dashed blue line contains the values calculated with the 20 spin chains. The dotted blue line is the classical $x^{1/2}$ spin wave approximation.[23] The inset compares the results obtained with finite chains of 11, 16, and 20 spins around x_0, with those given by eq A1 of the Appendix.

C_{mag}^{1D} approaches the spin wave limit. He obtained the coefficients of the polynomial by matching the curve and its first derivative to the finite chain approximation at a particular value of x, with the additional constraint that the total change of the molar magnetic entropy for a $S = {}^1/_2$ system should be R ln(2). Schlottmann[46,47] used the thermodynamic Bethe−Ansathz equations and obtained a similar dependence on $x^{3/2}$, but with an additional corrective term linear in x, having a negative coefficient.

We found useful obtaining a power expansion of C_{mag}^{1D} valid in a wide range of x, based on the 20 spin chains. For the low-temperature behavior of C_{mag}^{1D} we used the polynomials with three half integer terms (1/2, 3/2, 5/2) proposed by de Neef,[23] and with two half integer powers and a linear term (1/2, 1, 3/2) proposed by Schlottmann.[47] To perform the extrapolation, we least-squares-fitted these polynomials to the calculated C_{mag}^{1D} for a 20 spin chain in an interval $\Delta x = 0.2$, including 200 points around a value $x = x_o$; $x_o = 0.466$ was chosen imposing that the total change in the magnetic entropy calculated from the full curve amounts R ln(2). The best fit was obtained with the polynomial including the linear term,[46,47] and the result valid for $x < x_o$ is

$$\frac{C_{mag}^{1D}}{R} = 0.525(3)x^{1/2} - 0.702(6)x + 0.320(4)x^{3/2} \qquad (9)$$

By extrapolating to $N_S = \infty$ the values of C_{mag}^{1D} at each $x \geq x_o$ as a function of $1/N_S^2$, we obtain values of the specific heat identical to those obtained using the 20 spin chains. Thus, the variation with x of the specific heat of the FM chain obtained with eq 9 below x_o and with the 20 spin chains above x_o, plotted as a solid line in Figure 9 in log−log scale, leading to a total change $\Delta S_{mag}/R = 0.693(1)$ of the magnetic entropy (very close to ln(2)), describe accurately the specific heat in the range $0.001 < x < 20$. The dotted red straight line represents the classical spin wave limit,[3,23,26] and our results are compared with those of Blöte,[26] de Neef,[23] and Kondo and Yamaji.[48] To facilitate using our results to fit experiments, we constructed and describe in Appendix 1 an empirical function reproducing within 0.5% the values of $C_{mag}^{1D}(T)$ given in Figure 9.

Two parameters, $2J_0$ and the g factor, can be determined from the experimental results in the range where the magnetic behavior is 1D. The specific heat depends only on $2J_0$. The magnetization depends on both, $2J_0$ and g. To evaluate them we performed a global least-squares fit of eqs 6 and 8 to the specific heat and magnetization data for Cu(II)Tyr-Leu and Cu(II)Trp-Gly. To deal with the different magnitudes of the fitted properties, all values were normalized to the maximum of each property in the fitted interval. We excluded the experimental points below the temperature T_{1D} where the magnetic behavior is not 1D. Figures 10a,b and 11a,b show the data and the calculated curves which best fit simultaneously the specific heat and magnetization data for Cu(II)Tyr-Leu) and Cu(II)Trp-Gly, respectively. The least squares values, $2J_0/k_B = 3.60(5)$ K and $g = 2.106(6)$ for Cu(II)Tyr-Leu, and $2J_0/k_B = 2.59(5)$ K and $g = 2.086(6)$ for Cu(II)Trp-Gly, are included in Table 1. The residues of the global fit have a root-mean-square deviation smaller than 1% of the maximum values of the specific heat and the magnetization. The quoted uncertainties of $2J_0/k_B$ were estimated from the variance of the parameters for small changes in the fitted temperature intervals. The g-factors have an additional uncertainty due to the mass of the samples (±0.1 mg).

There is a large discrepancy between the value of $2J_0$ found here from the global fit for Cu(II)Trp-Gly ($2J_0/k_B = 2.59(5)$ K) and that reported before[17] obtained from only magnetic data. To understand this difference we calculated as a function of $2J_0$ and g the individual contributions to the standard deviation σ between the calculated and experimental values arising from the specific heat data (σ_C), and from the magnetic data (σ_M). We found that, close to the minimum of σ_M, there is a line in the (J_0, g) fitting parameter space, along which the value of σ_M

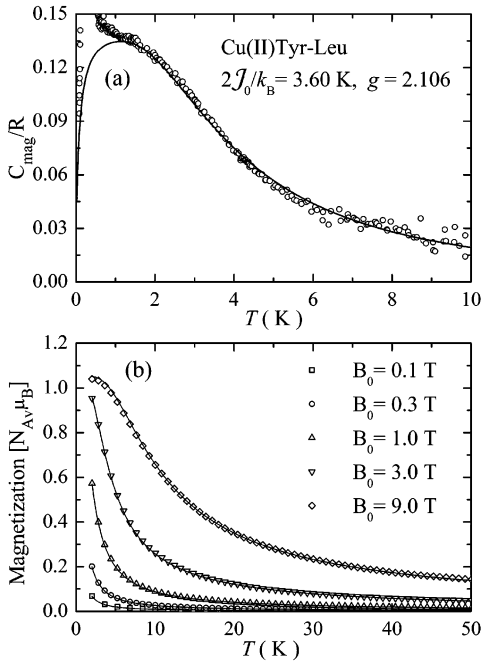

Figure 10. Results of the global fit of the specific heat data (to avoid cluttering only one-fourth of the experimental points are shown) (a) and magnetization data (b) for Cu(II)Tyr-Leu. The experimental results are compared with the values calculated with the parameters obtained from the global fit.

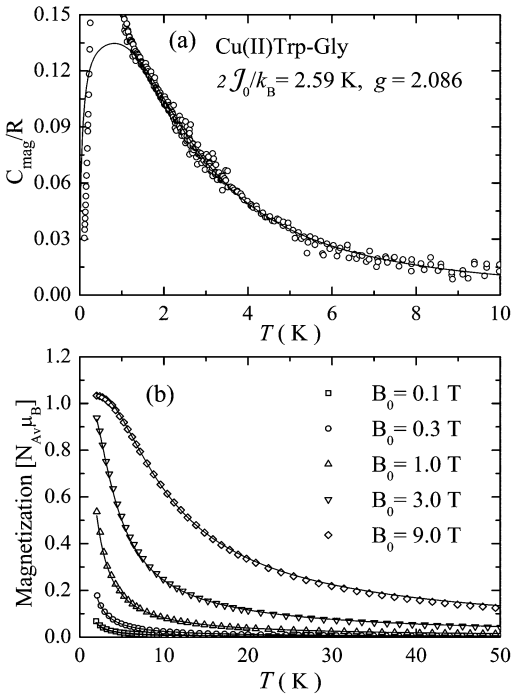

Figure 11. Results of the global fit of the specific heat (to avoid cluttering only one-fourth of the experimental points are shown) (a) and magnetization (b) data for Cu(II)Trp-Gly. The experimental results are compared with the values calculated with the parameters obtained from the global fit.

has a very small variation. This strong correlation of the fitting variables J_0 and g precludes an accurate determination of the parameters from a fitting of only magnetic data in order to obtain accurate values of $2J_0$. If the intrachain coupling $2J_0$ is evaluated by fitting the model only to magnetization data, a small improvement of the magnetization fit is obtained, at the cost of a poor prediction of the specific heat results. This is important and emphasizes the advantage of measuring the magnetic contribution to the specific heat in order to evaluate exchange interactions to study magnetostructural correlations and to compare values of $2J_0$ for compounds having similar exchange interaction paths.

Analysis of the ac Susceptibility Curves. In the linear response regime the complex ac susceptibility $\chi = \chi' - i\,\chi''$ is defined as the response of the magnetization $M_z(t)$ to a small oscillatory magnetic field $B(t) = B_0 + B_{ac}\exp(i\omega t)$ as[25,49]

$$M_z(t) = M_{zo} + \chi\, B_{ac}\exp(i\omega t) \tag{10}$$

A relaxation time τ is needed to establish thermal equilibrium between spins and lattice. If the frequency ω is much smaller than the spin−lattice relaxation rate $1/\tau$, $M_z(t)$ is in phase with the excitation, χ'' is negligible, and χ' equals the isothermal susceptibility χ_T given by

$$\chi_T(B_0,T) = \left(\frac{\partial M_z(B_0,T)}{\partial B_0}\right)_T = \frac{1}{k_B T}[\langle \mathcal{M}_z^2\rangle - \langle \mathcal{M}_z\rangle^2] \tag{11}$$

where M_z is defined in eq 7 and for $B_0 \to 0$, $\langle M_z\rangle \to 0$, and χ_T equals the standard dc susceptibility χ_o measured at small fields.[25] We calculated χ_T (B_0,T) using eq 11 and the values of $2J_0$ and g obtained from the global fit. The results are in good agreement with the static susceptibility data and with the values of $\chi'(B_0,T)$ measured for low applied dc magnetic fields (see Figure 7a,b). However, as shown in Figure 8a,b, a disagreement between the experimental values and those calculated for χ_T using eq 11 builds up as the applied dc magnetic field increases. For $B_0 \geq 1$ T the observed $\chi'(B_0,T)$ is smaller than the calculated isothermal susceptibility χ_T. According to the theory of Casimir and DuPre[49] (see Apendix 2) the relaxation time τ of the magnetization is described by

$$\tau = C_{mag}(B_0,T)/K \tag{12}$$

where K is the thermal conductivity relating the heat flow from the spin system to the lattice, to the temperature difference, ΔT, between spins and lattice ($dQ/dt = -K\,\Delta T$), and C_{mag} is the specific heat of the spin system. Equation 12 shows that τ follows the temperature and magnetic field variation of C_{mag}-(B_0,T) (eq 6). When $\omega\tau \ll 1$, $\chi' = \chi_T$ and $\chi'' = 0$. When $\omega\tau > 1$, $M_z(t)$ does not stay in thermal equilibrium with the lattice and $\chi' < \chi_T$. In the limit $\omega\tau \gg 1$, χ' equals the adiabatic susceptibility χ_S (Appendix 2). Away from the extreme cases, $\chi'(B_0,T)$ lies between $\chi_T(B_0,T)$ and $\chi_S(B_0,T)$.

To consider possible relaxation effects in the magnetization, we extended the global fit to all twelve curves for $C_{mag}(T)$, M_z-(B_0,T) and $\chi'(B_0,T)$, using $2J_0$, g, and K as fitting parameters, and the functional dependences of C_{mag}, χ_T, and χ_S as a function of B_0 and T from eqs 6, 11, and A4, respectively. The results of this global fit (not shown) are in reasonable agreement with the experimental values of χ' for all applied dc magnetic fields with values of the parameters $2J_0$ and g similar to those previously obtained. However, the values of $\chi''(B_0,T)$ calculated with these parameters are 2 orders of magnitude larger than the measured values (not shown). Also, and more important, a dependence of χ' with ω would be expected, in contrast with the experimental result. Thus, the disagreement between the ac susceptibility measured with large applied fields cannot be explained invoking a slow relaxation of the magnetization. Together with the experimental values of $\chi'(B_0,T)$, we display in Figure 8a,b the values calculated for the isothermal and adiabatic susceptibilities χ_T and χ_S of Cu(II)Tyr-Leu and Cu(II)-Trp-Gly. The differences between χ_T and χ_S at low T increase

rapidly with B_0; the data lie between the two curves at almost every T and B_0 (remember that J_o and g were fitted to C_{mag} and M_z only, not to χ').

Phase Transitions and Interchain Interactions. The very low T specific heat of Cu(II)Tyr-Leu) and Cu(II)Trp-Gly displayed in Figure 5a reflects the contribution of the magnetic excitations in the 3D-ordered spin system. The fitting of the data with a power law well below the transition temperatures leads to

$$\frac{C_{mag}}{R} = 6.5(9)T^{1.73(6)} \text{ for Cu(II)Tyr-Leu}$$

and

$$\frac{C_{mag}}{R} = 1.83(3)T^{1.84(1)} \text{ for Cu(II)Trp-Gly} \qquad (13)$$

One expects that, at the temperatures where the values in eq 13 were obtained, the SW approximation provides valid asymptotic expressions for the specific heat. Sorai and colleagues[50,51] gave expressions for a 3D Heisenberg magnet having different exchange parameters along the three directions. Since $2J_0 > 0$, and assuming equal exchange parameters $2J_1$ in the other two directions, it is obtained:

$$\frac{C_{mag}}{R} = \frac{5\zeta(5/2)\Gamma(5/2)}{16\sqrt{2}\pi^2 S^{1/2}} \frac{1}{\left(\frac{2J_0}{k_B}\right)^{1/2}\left(\frac{2J_1}{k_B}\right)} T^{3/2} \text{ for } J_1 > 0 \quad (14)$$

and

$$\frac{C_{mag}}{R} = \frac{\zeta(4)\Gamma(4)}{32\sqrt{2}\pi^2 S^3} \frac{1}{\left(\frac{2J_0}{k_B}\right)^{1/2}\left(\frac{|2J_1|}{k_B}\right)^{5/2}} T^3 \text{ for } J_1 < 0 \quad (15)$$

where $\zeta(z)$ and $\Gamma(z)$ are the Riemann zeta and Gamma functions, respectively. The temperature exponent of the magnetic specific heat obtained from the fitting to the data at very low temperature (eq 13) is closer to $T^{3/2}$ than T^3 for Cu(II) Trp-Gly. The fitting has a χ^2 value 1 order of magnitude larger for an exponent 3 than for 3/2. Also, the correlation coefficient for the 3/2 exponent is 0.97 versus the 0.7 obtained for a power of 3. Considering these facts and also from a visual inspection of the fittings, we conclude that the interchain exchange coupling $2J_1$ is FM for Cu(II)Trp-Gly and obtain $2J_1/k_B = 0.073(5)$ K. In the case of Cu(II)Tyr-Leu, this analysis is less conclusive because fittings using powers 3/2 and 3 are of similar quality. Thus, we calculated the values of $|J_1|$ assuming that the interchain interaction is either FM or AFM and obtained

$$2J_1/k_B = 0.015(2) \text{ K assuming } J_1 > 0$$

and

$$2J_1/k_B = -0.16(2) \text{ K assuming } J_1 < 0 \qquad (16)$$

Considering general thermodynamic concepts, Fisher[52] analyzed the relation between the specific heat and susceptibility of an antiferromagnet. He showed that the singular behavior of the specific heat of a simple AFM should follow the function $[\partial(\chi T)/\partial T]$ involving the derivative of the susceptibility χ. Thus, the temperature of the peak appearing in the susceptibility at a 3D magnetic transition should be higher than the temperature of the corresponding peak in the specific heat. We do not know about similar predictions in the case of simple FM. Since the compounds studied here have g anisotropy ($\sim$10%)[17,34,35] and rotated copper molecules, they are not expected to have "simple" behavior, and it is difficult to discuss the temperatures of the peaks. Experimentally, for Cu(II)Trp-Gly they are very close but for Cu(II)Tyr-Leu, with a lower transition temperature, the measurement of the temperature of the sample is not accurate enough to make a comparison (see Experimental section).

Discussion

Magnitudes of the Exchange Interactions. *The Intrachain Exchange Interactions.* In the previous analysis we showed that specific heat data are most appropriate to evaluate the intrachain exchange interactions for FM 1D chains. Since the specific heat depends only on the exchange parameter $2J_0$, the quality of the fits is not affected by cross correlations between parameters of the model. This occurs with the magnetization, which depends on $2J_0$ and on the g factor of the magnetic ions. This fact is not usually recognized. The values for the intrachain exchange interaction (Table 1) obtained here from a global fit of the model to the specific heat and magnetization data reproduce very well both sources of data (see Global Fitting section).

In most cases the coupling transmitted by the helix-like equatorial−equatorial syn-anti carboxylate bridges similar to those reported first by Freeman et al.[20] is FM, [10−19] and a qualitative explanation has been given by Colacio et al.[10] However, no quantitative analysis of the correlation between the structural parameters and the magnitude of the coupling $2J_0$ has yet been reported.

As described in the structural section, the main difference between the intrachain exchange paths Cu−O−C−O−Cu is in one of the torsion angles which amounts 16.5° for Cu(II)Trp-Gly and only −0.4° for Cu(II)Tyr-Leu. To rationalize how this torsion angle affects the value of $2J_0$, we tried to calculate the modification of the antiferromagnetic contribution considering the value of $(\epsilon_- - \epsilon_+)$, being $\epsilon\pm$ the energies of the bonding/antibonding combinations of the magnetic orbitals in the triplet state.[1,53,54] We found that the small value of the variation of this quantity with the torsion angle precludes obtaining a meaningful trend from the electronic structure calculation.

We also analyzed the possible role of the angle subtended by the basal planes of the copper ions linked by the carboxylate bridge.[19] The values of this angle for Cu(II)Tyr-Leu and Cu(II)Trp-Gly are, respectively, 25.6 and 31.9°, very different from the corresponding angles (72.6−80.5°) in the bridges of the compounds studied by Pasán et al.[19] Nevertheless, in both cases the interaction is FM. We conclude that more experimental results obtained with the same model and experimental method (preferently including specific heat measurements) are needed to obtain a meaningful quantitative magnetostructural correlation.

The Interchain Exchange Interactions and the Temperature of the Phase Transition. The analysis of the specific heat data below the 3D phase transition temperature for Cu(II)Trp-Gly using spin-wave theory allowed to estimate a magnitude $2J_1/k_B = 0.073(5)$ K for the ferromagnetic exchange interaction between copper ions in neighbor chains following Sorai and colleagues.[50,51] Considering the important differences underlaying the basic concepts of the two methods, this result compares well with the value $|2J_1/k_B| = 0.061(2)$ K measured previously using EPR.[17] This exchange interaction is associated with the interchain bridge provided by paths I and II described in Figures 2a, 3b, and 3c, all containing cation−π contacts. Because of

the shorter distance of the cation−π contact, we propose that path I is more effective than path II. This assumption cannot be proved.

An equivalent calculation using the specific heat data for Cu(II)Tyr-Leu does not give a clear answer because the spin wave model does not allow in this case to distinguish 3D FM from 3D AFM behavior below the phase transition. Assuming FM interaction, we obtained $2J_1/k_B = 0.015(2)$ K while assuming AFM interaction the result is $2J_1/k_B = -0.16(2)$ K, 1 order of magnitude different. Another source of experimental information is needed to support one of these values. Performing EPR experiments for Cu(II)Tyr-Leu similar to those in ref 17 for Cu(II)Trp-Gly, we obtained[34,35] $|2J_1/k_B| = 0.016$ K which, compared with the values given above, indicates that the exchange interaction between Cu ions in neighbor chains in Cu(II)Tyr-Leu is FM and $2J_1/k_B = 0.015(2)$ K. This exchange interaction is associated with the interchain path containing 12 diamagnetic atoms with a total length of 19.09 Å described in Figures 1a and 3a.

The ferromagnetic exchange interactions discussed above are responsible for the 3D magnetic transitions observed at 0.16 K for Cu(II)Tyr-Leu and 0.53 K for Cu(II)Trp-Gly. Considering that the values of the intrachain interaction $2J_0$ for both compounds are similar, one observes that the ratio of the transition temperatures obtained from the position of the low-temperature peaks of the specific heat is similar to the ratio between the interchain interactions occurring in the plane perpendicular to the chains. This reasonable result gives further support to the evaluation of the interchain exchange interactions presented above.

One may argue that eqs 14 and 15 correspond to simple 3-D Heisenberg systems and do not take into account the particular topology of the interchain exchange paths for these compounds. As considered by Ohmae et al.[51] this fact along with the very different magnitudes of the intra- and interchain exchange interactions could produce a dimensional crossover invalidating eqs 14 and 15, and the conclusions regarding the interchain exchange interactions as FM or AFM should be revised. However, the agreement between the values obtained here for $2J_1$ with those obtained from EPR and with the ratio between the temperatures of the phase transition support the results presented here, which are included in Table 1. An alternative procedure to that of refs 50 and 51 to obtain the value of $2J_1$ has been recently proposed by Yasuda et al.[55] for the case of AFM chains and layers, using the 3D transition temperature and the value $2J_0$. Despite some similarities present in that transition and in our FM chain systems, we consider the approach not directly applicable to our case.

The meaning of FM interactions through the long interchain chemical bridges occurring in Cu(II)Tyr-Leu and Cu(II)Trp-Gly is an interesting result that has to be investigated further theoretically and experimentally in other similar systems.

To end up with our analysis of the interchain interactions, we want to emphasize that measurement of exchange interactions transmitted through biologically relevant chemical bridges as those shown in Figure 3a,b,c for Cu(II)Tyr-Leu and Cu(II)-Trp-Gly is important. As it has been shown by several authors,[56−61] the exchange coupling parameter is related to the matrix element for electron-transfer processes along the path. Their values provide a way to estimate these matrix elements, which are very difficult to calculate by other methods. Thus magnetic studies of model compounds as those reported here provide information useful to understand electron transfer in proteins, where similar chemical bridges occur.

ac Magnetic Susceptibility in the Presence of an Applied dc Field. The experimental values of the real part of the ac susceptibility of Cu(II)Tyr-Leu and Cu(II)Trp-Gly observed under small applied dc fields are equal to the static susceptibility. They are reproduced by the isothermal or static susceptibility χ' calculated using eq 11 and the values of $2J_0$ and g obtained from the global fit of the specific heat and magnetization data. However, χ' observed in the presence of large applied fields ($B_0 > 1$ T) greatly differ from the isothermal susceptibility predicted by eq 11, which already considers the effect of a nonlinear magnetic response due to magnetization saturation in the presence of the large magnetic fields. For all magnetic fields, the observed susceptibility values are between those predicted for the isothermal and for the adiabatic susceptibility. However, neither the frequency dependence of $\chi'(B_0,T)$ nor the values of $\chi''(B_0,T)$ follow the predictions of the theory of Casimir and DuPre[49] for the ac susceptibility of a slow relaxing magnetization. This disagreement was already observed for the susceptibility of Cu(II)Trp-Gly.[17] We do not have an explanation for this observation and are not aware of reports of similar problems in the analysis of ac susceptibilities measured in the presence of large applied dc fields.

Acknowledgment. The authors would like to thank CNPq, FAPERJ and CAPES in Brazil and ANPCyT PICT 06-13872, PIP 5274, and CAI+D-UNL in Argentina for financial support. A multinational grant of the Antorchas Foundation made possible this collaboration. The authors acknowledge the Spanish Research Council (CSIC) for providing a free of charge license to the CSD system.[21,22] D.E.R. and R.C. are members of CONICET. We are grateful to Prof. Henk Blöte for useful suggestions.

Appendix 1: Functional Dependence of the Specific Heat of FM Chains

Numerical functions calculated from values of the thermodynamic variables obtained from models are useful to fit experimental data. Hatfield,[62] reported an empirical equation reproducing the temperature variation of the magnetic susceptibility of AFM chains for $x > 0.05$ generated from calculations on chains of ten $S = 1/2$ spins. To calculate an empirical function reproducing the specific heat of AFM chains, Rapp et al.[63] used the eigenvalues of 16 spin chains reported by Fabricius et al.[24] In this work we used the values of the specific heat as a function of $x = k_BT/J_0$ ($B_0 = 0$) calculated as described in the text (see Figure 9) to obtain an empirical function reproducing the calculated specific heat of a FM chain better than 0.5% in the range $0.001 < x < 10$. This 4-orders-of-magnitude range in x requires the use of the variable $z = \log(x)$. The function is

$$\log[C_{mag}(z)] = \frac{b_1 + b_2z + b_3z^2 + b_4z^3 + b_5z^4 + b_6z^5}{1 + c_1z + c_2z^2 + c_3z^3 + c_4z^4 + c_5z^5} \quad \text{(A1)}$$

We obtained $b_1 = -0.89001(2)$, $b_2 = 0.173(5)$, $b_3 = -3.283(6)$, $b_4 = -1.62(1)$, $b_5 = -1.735(4)$, $b_6 = -0.481(4)$, $c_1 = -0.464(6)$, $c_2 = 2.720(8)$, $c_3 = 0.11(1)$, $c_4 = 0.124(2)$, $c_5 = 0.1152(9)$. Equation A1 can be used to fit specific heat data for 1D FM in order to calculate the exchange interaction parameter $2J_0$ defined in eqs 1 and 2, and was used to draw the solid lines in Figures 10a and 11a.

Appendix 2: Slow Relaxation of the Magnetization

According to Casimir and DuPre,[49] and assuming exponential relaxation with a single spin−lattice relaxation time τ needed

to establish thermal equilibrium between the chain magnetization and the lattice, the real and imaginary parts of the ac susceptibility χ' and χ'' depend on the frequency ω of the measurement and on the relaxation time τ as

$$\chi'(\omega) = \frac{\chi_T - \chi_S}{1 + \omega^2\tau^2} + \chi_S \quad \text{(A2)}$$

$$\chi''(\omega) = \frac{\omega\tau}{1 + \omega^2\tau^2}(\chi_T - \chi_S) \quad \text{(A3)}$$

where χ_T and χ_S are the isothermal and adiabatic susceptibilities. In this theory $\tau = C_{mag}(B_0,T)/K$, where K is the thermal conductivity ($dQ/dt = -K\Delta T$).[49] If τ is short ($\omega\tau \ll 1$), the spin temperature and the magnetization respond immediately to the applied field, e.g., the populations of the energy levels obey at all times a Boltzmann distribution with the temperature of the thermal bath, $M_z(t)$ and $B_{ac}(t)$ are in phase, $\chi'' = 0$ and χ' is equal to the static or isothermal susceptibility $\chi_o = \chi_T$. When $\omega\tau \gg 1$, the populations of the levels remain constant during the field modulation cycle and there is not thermal equilibrium between spins and bath. In this extreme case χ' equals the adiabatic susceptibility χ_S, and $\chi'' = 0$. As obtained from eqs A2 and A3, for intermediate values of $\omega\tau$, χ' changes from χ_T to χ_S, while χ'' has a maximum value

$$\chi''(\omega) = \frac{\chi_T - \chi_S}{2}$$

for $\omega\tau = 1$. Equations A2 and A3 and measurement of χ' and χ'' as a function of temperature and magnetic field in a wide range of frequency ω could allow to obtain χ_T, χ_S and the relaxation time τ. Also, one could calculate χ_T and χ_S with a magnetic model and use eqs A2 and A3 to estimate τ from measured values of χ' and χ''. The adiabatic susceptibility $\chi_S(B_0,T) = (\partial M_z/\partial B)_s$ can be calculated using the thermodynamic identity:

$$\chi_S = \chi_T - T\frac{\eta_{B_0}^2}{C_{mag}(B_0,T)} \quad \text{(A4)}$$

where C_{mag}, defined in eq 6, has to be calculated with the applied magnetic field. The change of the magnetization with temperature at constant field η_{B_0} is obtained by derivation of eq 8:

$$\eta_{B_0} = -\left(\frac{\partial M_z(B_0,T)}{\partial T}\right)_{B_0} = \frac{N_{Av}}{k_B N_S T^2}[\langle \mathscr{H}\mathscr{M}\rangle - \langle \mathscr{H}\rangle\langle \mathscr{M}\rangle] \quad \text{(A5)}$$

According to eq A4, in all cases is $\chi_S < \chi_T$.

References and Notes

(1) Kahn, O. *Molecular Magnetism*; VCH: New York, 1993.

(2) Mattis, D. C. *The Many-Body Problem. An Encyclopedia of Exactly Solved Models in One Dimension*; World Scientific: Singapore, 1993.

(3) Bonner, J. C.; Fisher, M. E. *Phys. Rev.* **1964**, *135*, A640−658.

(4) De Jongh, L. J.; Miedema, A. R. *Adv. Phys.* **1974**, *23*, 1−260.

(5) Griffiths, R. B. *Phys. Rev.* **1964**, *135*, A659−660.

(6) We define the exchange interaction between spins $\mathbf{S}_i$ and $\mathbf{S}_j$ as $\mathscr{H}_{ex}(i,j) = -2J_{ij}\,\mathbf{S}_i\cdot\mathbf{S}_j$, as classically used to describe spin chains [ref 3]. This definition differs from that frequently used in molecular magnetism, $\mathscr{H}_{ex}(i,j) = -\mathscr{J}_{ij}\,\mathbf{S}_i\cdot\mathbf{S}_j$ [ref 1], where $2J_{ij}$ is replaced by $\mathscr{J}_{ij}$. In a dinuclear unit of $^1/_2$ spins $2J_{ij} = \mathscr{J}_{ij}$ corresponds to the singlet−triplet splitting.

(7) Bleaney, B.; Bowers, K. D. *Proc. R. Soc. A London* **1952**, *214*, 451−465.

(8) Carlin, R. L.; Kopinga, K.; Kahn, O.; Verdaguer, M. *Inorg. Chem.* **1986**, *25*, 1786−1789.

(9) Levstein, P. R.; Calvo, R. *Inorg. Chem.* **1990**, *29*, 1581−1583.

(10) Colacio, E.; Costes, J. P.; Kivekas, R.; Laurent, J. P.; Ruiz, J. *Inorg. Chem.* **1990**, *29*, 4240−4246.

(11) Colacio, E.; Dominguez-Vera, J. M.; Costes, J. P.; Kivekas, R.; Laurent, J. P.; Ruiz, J.; Sundberg, M. *Inorg. Chem.* **1992**, *31*, 774−778.

(12) Nanda, K. K.; Addison, A. W.; Sinn, E.; Thompson, L. K. *Inorg. Chem.* **1996**, *35*, 5966−5967.

(13) Schulz, D.; Weihermüller, T.; Wieghartdt, K.; Butzlaff, C.; Trautwein, A. X. *Inorg. Chim. Acta* **1997**, *247*, 387−394

(14) Chen, P.; Liao, D.; Yan, S.; Jiang, Z.; Wang, G.; Yaop, X.; Wang, H. *Inorg. Chim. Acta* **1997**, *254*, 371−373.

(15) Colacio, E.; Ghazi, M.; Kivekas, R.; Moreno, J. M. *Inorg. Chem.* **2000**, *39*, 2882−2890.

(16) Colacio, E.; Domínguez-Vera, J. M.; Ghazi, M.; Kivekas, R.; Klinga, M.; Moreno, J. M *Eur. J. Inorg Chem.* **1999**, 441−445.

(17) Costa-Filho, A. J.; Nascimento, O. R.; Ghivelder, L.; Calvo, R. *J. Phys. Chem. B* **2001**, *105*, 5039−5047.

(18) King, P.; Clérac, R.; Anson, C. E.; Copulon, C.; Powell, A. K. *Inorg. Chem.* **2003**, *42*, 3492−3500.

(19) Pasán, J.; Delgado, F. S.; Rodríguez-Martín, Y.; Hernández-Molina, M.; Ruiz-Perez, C.; Sanchiz, J.; Lloret, F.; Julve, M. *Polyhedron* **2003**, *22*, 2143−2153.

(20) Freeman, H. C.; Healy, M. J.; Scudder, M. L. *J. Biol. Chem.* **1977**, *252*, 8840−8857.

(21) Allen, F. H. *Acta Crystallogr*. **2002**, *B58*, 380−388.

(22) Bruno, I. J.; Cole, J. C.; Edington, P. R.; Kessler, M.; Macrae, C. F.; McCabe, P.; Pearson, J.; Taylor, R. *Acta Crystallogr*. **2002**, *B58*, 389−397.

(23) De Neef, T. *Phys. Rev. B* **1976**, *13*, 4141−4158.

(24) Fabricius, K.; Löw, U.; Mutter, K. H.; Ueberholz, P. *Phys. Rev. B* **1991**, *44*, 7476−7485.

(25) Carlin, R. *Magnetochemistry*; Springer: Berlin, 1986.

(26) Blöte, H. W. J. *Physica* **1974**, *78*, 302−307.

(27) Willet, R. D.; Gaura, R. M.; Landee, C. P. In *Extended Linear Chain Compounds*; Miller, J. S., Ed.; Plenum: New York, 1983; Vol. 3; pp 143−191.

(28) Jeffrey, G. A.; Saenger, W. *Hydrogen Bonding in Biological Structures*; Springer: Berlin, 1991.

(29) Jeffrey, G. A. *An Introduction to Hydrogen Bonding*; Oxford University Press: New York, 1997.

(30) Dougherty, D. A. *Science* **1996**, *271*, 163.

(31) Ma, J. C.; Dougherty, D. A. *Chem. Rev.* **1997**, *97*, 1303.

(32) Keefer, F. In *Ferromagnetism*; Flugge, S., Ed.; Springer: Berlin, 1966; Vol. XVIII/2; pp 1−273.

(33) Kittel, C. *Introduction to Solid State Physics*, 3rd ed.; Wiley: New York, 1968; Chapter 6.

(34) Casado, N. M. C., Ph.D. Thesis, FBCB, Universidad Nacional del Litoral, Argentina, 2002.

(35) Casado, N. M. C.; Santana, R. C.; Baggio, R.; Rapp, R. E.; Calvo, R. In preparation.

(36) Baggio, R.; Casado, N. M. C.; Calvo, R.; Rapp, R. E.; Garland, M. T. *Acta Crystallogr*. **2005**, *C61*, m250−252.

(37) Nascimento, O. R.; Costa, A. J.; DeMorais, D. I.; Ellena, J.; Delboni, L. F. *Inorg. Chim. Acta* **2001**, *312*, 133−138.

(38) Siqueira, M. L.; Rapp, R. E.; Calvo, R. *Phys. Rev. B* **1993**, *48*, 3257−3263.

(39) Calvo, R.; Passeggi, M. C. G.; Moreno, N. O.; Barberis, G. E.; Braun-Chaves, A.; Torres, B. C. M.; Lezama, L.; Rojo, T. *Phys. Rev. B* **1999**, *60*, 1197−1203.

(40) Torikachvili, M. S.; Yang, K. N.; Calvo, R.; Nascimento, O. R.; Maple, M. B. *Cryogenics* **1983**, *23*, 52−54.

(41) Martin, D. L.; Bradley, L. L. T.; Cazemier, W. J.; Snowdon, R. L. *Rev. Sci. Instrum.* **1973**, *44*, 675−684.

(42) Swenson, C. A. *Rev. Sci. Instrum.* **1999**, *70*, 2728−2731.

(43) *International Tables for X-ray Crystallography. Vol. A. Space-Group Symmetry*; Hahn, T., Ed. Reidel: Dordrecht, 1987; Vol. A.

(44) Sakabikara, T.; Miyazaki, Y.; Ishida, T.; Nogami, T.; Sorai, M. *J. Phys. Chem. B* **2002**, *106*, 6390−6394.

(45) The small distortions of the magnetization curves around 55 K in Figure 6 are experimental artifacts introduced when subtracting the contribution of the sample holder, as a consequence of small temperature shifts of the measurements of the sample and the empty holder.

(46) Schlottmann, P. *Phys. Rev. Lett.* **1985**, *54*, 2131−2134.

(47) Lee, K. J. B.; Schlottmann, P. *Phys. Rev. B* **1987**, *36*, 466−473.

(48) Kondo, J.; Yamaji, Y. *Prog. Theor. Phys.* **1972**, *47*, 807−818.

(49) Casimir, H. B.; Du Pre, F. K. *Physica* **1938**, *5*, 507−511. See also, Gorter, C. J. *Paramagnetic Relaxation*; Elsevier: New York, 1947. Cooke, A. H. *Rep. Prog. Phys.* **1950**, *13*, 276−294. Pake, G. E. *Paramagnetic Resonance*; Benjamin, **1962**, ch. 6. Poole, C. P.; Farach, H. A. *Relaxation in Magnetic Resonance. Dielectric and Mössbauer Applications*; Academic Press: New York, 1971; ch. 18.

(50) Matsumoto, T.; Miyazaki, Y.; Albrecht, A. S.; Landee, C. P.; Turnbull, M. M.; Sorai, M. *J. Phys. Chem. B* **2000**, *104*, 9993−10000.

(51) Ohmae, N.; Kajiwara, A.; Miyazaki, Y.; Kamachi, M.; Sorai, M. *Thermochim. Acta* **1995**, *267*, 435−444.
(52) Fisher, M. E. *Philos. Mag*. **1962**, *7*, 1731−1743.
(53) Hay, P. J.; Thibeault, J. C.; Hoffmann, R. H. *J. Am. Chem. Soc.* **1975**, *97*, 4884−4899.
(54) Kahn, O. In *Magneto-Structural Correlations in Exchange Coupled Systems*; R. D. Willet et al., Eds.; Reidel: Dordrecht, 1985; pp 37−56.
(55) Yasuda, C.; Todo, S.; Hukushima, K.; Alet, F.; Keller, M.; Troyer, M.; Takayama, H. *Phys. Rev. Lett*. **2005**, *94*, 217201.
(56) Okamura, M. Y.; Isaacson, R. A.; Feher, G. *Biochim. Biophys. Acta* **1979**, *546*, 394−417. Okamura, M. Y.; Fredkin, D. R.; Isaacson, R. A.; Feher, G. *Quantum Mechanical Tunneling in Biological Systems*; Chance, B., DeVault, D. C., Frauenfelder, H., Marcus, R. A., Suttin, N., Eds.; Academic Press: New York, pp 729−743, 1979.
(57) De Vault, D. C. *Quantum Mechanical Tunneling in Biological Systems*; Cambridge University Press: London, pp 118−121, 1984.
(58) Bominaar, E. L.; Achim, C.; Borshch, S. A.; Girerd, J. J.; Münck, E. *Inorg. Chem*. **1997**, *36*, 3689−3701.
(59) Calvo, R.; Abresch, E. C.; Bittl, R.; Feher, G.; Hofbauer, W.; Isaacson, R. A.; Lubitz, W.; Okamura, M. Y.; Paddock, M. L. *J. Am. Chem. Soc.* **2000**, *122*, 7327−7341.
(60) Chen, P.; Solomon E. I. *Proc. Natl. Acad. Sci. U.S.A.* **2004**, *101*, 13105−13110.
(61) Weiss, E. A.; Wasielewski, M. R.; Ratner, M. A. *J. Chem. Phys*. **2005**, *123*, 064504.
(62) Hatfield, W. E. *J. Appl. Phys*. **1981**, *52*, 1985−1990.
(63) Rapp, R. E.; de Souza, E. P.; Godfrin, H.; Calvo, R. *J. Phys.: Condens. Matter* **1995**, *7*, 9595−9606.